Struct Multidisc Optim (2017) 56:435–453
DOI 10.1007/s00158-017-1673-9

INDUSTRIAL APPLICATION

An optimization study on load alleviation techniques in gliders using morphing camber

José Vale[1] · Frederico Afonso[1] · Éder Oliveira[1] · Fernando Lau[1] · Afzal Suleman[1,2]

Received: 2 December 2016 / Revised: 22 January 2017 / Accepted: 15 February 2017 / Published online: 14 March 2017

Abstract This study explores wing morphing for load alleviation as a means to reduce the required wing structural weight without compromising aircraft performance. A comparative study between the lift-to-drag ratio (L/D) performance of a fixed wing glider (FWG) and a cambered morphing wing glider (CMWG) is presented. Both aircraft are aero-structurally optimized for the best L/D for a given speed and payload mass. A combination of lifting-line theory and 2D viscous calculations is used for the aerodynamics and an equivalent beam model is employed for the structural analysis. Pull-up and -down maneuvers at 25 m/s and near stall angle of attack are assumed as critical load cases. Results of the FWG optimization are shown for several trimmed flight conditions with varying mass and velocity. Results are compared to the ones from the CMWG optimization and conclusions are drawn on the improvement in the L/D ratio throughout the flight envelope and on potential reductions in the wing structural mass due to the load alleviation strategy. The wing camber adaptation provides significant performance gains in a large range of flight speeds with negligible penalties in the low speeds range. However, maneuverability is penalized.

✉ José Vale
zevale@tecnico.ulisboa.pt

[1] CCTAE, IDMEC, Instituto Superior Técnico, Universidade de Lisboa, Av. Rovisco Pais, No. 1, 1049-001 Lisboa, Portugal

[2] Department of Mechanical Engineering, University of Victoria, PO Box 1700, Stn. CSC, Victoria, BC V8W 2Y2, Canada

Keywords Morphing glider · Multidisciplinary design optimization · Load alleviation · Flight performance

Nomenclature

AOA	Angle of attack
AOA_{max}^{HT}	Maximum horizontal tail's angle of attack
AOA_{max}^{wing}	Maximum wing's angle of attack
Ar	Wing aspect ratio
C	Chord
C_d	2D drag coefficient
C_D	Drag coefficient
C_l	2D lift coefficient
C_L	Lift coefficient
C_{L_α}	Lift curve slope
C_m	2D pitch moment coefficient
C_M	Pitch moment coefficient
CG	Center of gravity
CGx	CG position in the aircraft's longitudinal axis
D	Total drag
CMWG	Camber morphing wing glider
EB	Equivalent beam
FWG	Fixed wing glider
g	Gravity acceleration
HT	Horizontal tail
L	Total lift
L/D	Lift-to-drag ratio
L/W	Load factor
LLT	Prandtl's lifting line theory
PFS	Front spar position relative to chord
PRS	Rear spar position relative to chord
Re	Reynolds number
SF	Structural safety factor
SM	Static margin

TFS	Front spar thickness
TLS	Lower skin thickness
TRS	Rear spar thickness
TUS	Upper skin thickness
W	Total weight
W_1	Objective function weight 1
W_2	Objective function weight 2
W_{payload}	Payload weight
W_{wing}	Wing weight
y	Spanwise position
θ	Angle of twist
$\sigma_{max}^{pull-down}$	Maximum stress for a pull-down maneuver
$\sigma_{max}^{pull-up}$	Maximum stress for a pull-up maneuver
σ_{max}	Maximum stress
σ_{yield}	Material yield strength

1 Introduction

Several attempts have been made to determine if morphing concepts are beneficial solutions for flight efficiency improvement. Design frameworks have been proposed at a conceptual level by Wittmann (2014) and Cesnik et al. (2004) as well as morphing strategy optimization methodologies (Yoon 2013). Nevertheless, the reported morphing concepts studies seldom include all the necessary interdisciplinary coupling to provide clear metrics for comparison and the majority of the work reported on the subject lacks proper evaluation of all the benefits and penalties involved, which include, but are not restricted to aerodynamic efficiency (including fuselage and trim drag), mass increase and stability/maneuverability.

Morphing concepts proposed and studied include the variable span (Santos et al. 2015; Vale et al. 2011), variable camber (Molinari et al. 2011; De Gaspari et al. 2014; Dayyani and Friswell 2016), variable twist (Pecora et al. 2012; Werter et al. 2016) wings and morphing wingtip/winglets (Cooper et al. 2015; Falcão et al. 2011) are just some examples of the most common wing geometrical parameters used to optimally adapt the wing geometry to the flight conditions.

The concept of camber morphing in airfoils is already a reality through the use of flap devices for lift augmentation. The flaps allow adaptation of the aircraft to different flight conditions, namely take-off and landing. Other than that, camber morphing (as other morphing concepts) generally fails to provide significant benefits for aircraft when missions do not include significant changes in flight conditions. Nowadays, the level of optimization of conventional aircraft configurations performing nearly constant cruise flight segments that represent most of the flight mission does not leave space for improvement.

Camber morphing can be used for load alleviation of the wing structure when subjected to wind gusts or maneuvering, leading to potential savings in wing structural mass. Load alleviation (Regan and Jutte 2012) is usually addressed using the control surfaces and control algorithms to reduce the aerodynamic loads during the occurrence of the disturbance in the flight conditions (Matsuzaki et al. 1989; Mangalam et al. 2008; Shao et al. 2010), but the capability of the control surfaces to control the loading distribution is somewhat limited. A different approach by Haftka (1977) demonstrated the advantage of composite wings over alumninum ones in their ability to deform into load-alleviating shapes in high-g maneuvers. His study provides an example of how structural weight reduction can be obtained with proper design of the wing structure for load alleviation during critical maneuvers.

This paper explores the possibility of using a camber morphing wing capable of active spanwise camber variation in order to reduce wing structural mass during high load situations, by changing the load distribution and its magnitude, while either maintaining the performance of the aircraft unaffected or further improving it.

The engineering innovation of this work is based on the evaluation of the actual structural wing weight benefit and its effect on the overall aircraft performance using a camber morphing concept. The performance is compared to a baseline constant geometry wing aircraft. Additionally, the evaluation of the aerodynamic benefits of camber morphing while enabling significant load alleviation is also a novel aspect of the paper.

In this work, Multidisciplinary Design Optimization (MDO) is used to design an optimal Fixed Wing Glider (FWG) for maximum range (maximum L/D) with a constant shape airfoil and span (1m), for a specific payload mass and airspeed and calculate its performance within its flight envelope. These results are then compared to the ones obtained for an optimized Camber Morphing Wing Glider (CMWG) for the same payload and flight conditions.

The FWG is optimized in a single level optimization scheme while the CMWG is optimized using sequential optimization and surrogate model with a sample updating scheme. Both aircraft are optimized taking into to account not only aerodynamic and structural considerations but also static stability considerations, for which the wing mass plays a significant role. Structural wing mass, actuation and morphed configurations for several flight conditions are calculated and the quantitative assessment of the benefits of the CMWG relatively to the FWG is performed and discussed.

The choice for a glider comparison was driven by two main factors: a reduction in problem complexity due to the absence of propulsion and consequently not needing an accurate description of propulsion efficiency and consumption; usually the performance of a flapped glider at the design point is worse than if its airfoils are optimized without

considering the flap, therefore using morphing as an adaptation strategy may improve the performance in off-design conditions without penalizing the on-design performance.

In Section 2, the MDO procedure is described for the optimization of both the FWG and the CMWG. Section 3 presents the final designs results. Section 4 compares the on-design performance and describes the performance results in off-design conditions and discusses the advantages and disadvantages of using such a camber morphing wing. Finally, the Conclusions and Future Work sections outline the main findings and possible research paths from the actual point of this work.

2 Multidisciplinary design optimization of the FWG and CMWG

Multidisciplinary design optimization is used for the design of both aircraft. Based on the design requirements and operational limits described below an MDO problem is devised to obtain the design that maximizes the L/D ratio of the aircraft while still maintaining the wing's structural integrity during the limit load maneuvers. The disciplines involved in the MDO procedure for both the FWG and the CMWG are Aerodynamics, Structures and Static Stability.

2.1 Design and performance requirements

The purpose of this study is to assess if there are benefits in considering the design of a camber morphing wing instead of a fixed wing in a small scale glider. The benefits are assessed essentially in three distinct metrics: 1) Expansion of the flight envelope; 2) Improvement in L/D performance (including trim drag) and; 3) Reduction of wing structural weight through load alleviation.

The starting point for the design is a design payload mass of 0.225 Kg, a design flight speed of 7.5 m/s and a design altitude of 0 m. Altitude variations are neglected.

It is assumed that the payload mass includes all components of the aircraft except the wing structure. As a consequence of this assumption, actuation systems for the CMWG are being included in the payload, as are the unaccounted parts of the FWG wing (leading and trailing edge structures) and aileron actuation systems. Also the Horizontal Tail (HT) mass is being included in the payload. Thus, any effects of HT size in both aircraft mass are unaccounted for, which may mean extra benefits from CMWG if this aircraft HT size is lower than the FWG HT size. Fixed aircraft dimensions are the span (1 m), the distance between main wing and HT leading edges (0.5 m) and the HT span (0.2 m). Both lifting surfaces have unswept leading edges.

Limiting operation conditions are the maximum flight speed of 25 m/s and local Angle of Attack (AOA) equal to $\pm 10°$. As the limit load cases, pull up and down at 25 m/s are considered. These load cases are assumed to be represented by the steady lift distributions obtained at the referred speed with a $\pm 10°$ AOA, respectively.

The wing structure is assumed to be of an isotropic rigid polymeric material, capable of being molded into low thickness structures and allow thickness variations along the structural components. The structural safety factor (SF) was arbitrarily defined as 1.25.

Stability requirements are imposed as a static margin lower limit of 10%. Table 1 summarize the information described above.

2.2 Aerodynamics

The aerodynamic calculations of both aircraft are based on previously computed airfoil aerodynamic coefficients databases using a panel code coupled with viscous boundary layer equations (Hepperle 2007), in a similar approach to what is used in XFOIL (Drela 1989). The 2D lift, drag and pitching moment coefficients (C_l, C_d and C_m respectively) are calculated for several values of AOA and Reynolds number (Re) for the different airfoil shapes obtained from the structural optimization for the CMWG, as will be discussed in the next subsection, or for the chosen airfoil to be used in the main wing of the FWG.

Given the values of local chord, local incidence and local C_L vs AOA curve slope at several wing stations, the Prandtl's Lifting Line Theory (LLT) (Houghton and Carpenter 2001) is used to obtain the effective AOA for each wing station. The effective AOA in turn is used together with the local Re and the airfoil shape parameter (in the CMWG case only) to obtain the local 2D aerodynamic coefficients, through interpolation of the created databases.

Finally, the C_l, C_d and C_m distributions are integrated along the wing span to obtain their three dimensional counterparts C_L, C_D and C_M, respectively.

Table 1 Summary of design and performance requirements

Item	Quantity
Design payload	0.225 Kg
Design flight speed	7.5 m/s
Design Altitude	0 m
Span	1 m
Distance between main wing and HT	0.5 m
HT Span	0.2 m
Maximum flight speed	25 m/s
Max/Min local AOA	$10°/-10°$
Static Margin	$>10\%$
Limit load cases conditions	25 m/s; $\pm 10°$ AOA
Structural material density	1160 Kg/m^3
Max. Tensile/Compressive stress	40 MPa /−40 MPa
Structural Safety Factor (SF)	1.25

This approach is justifiable due to the expected relatively high Aspect Ratio (Ar) of the wings to be obtained. The wing sections are then assumed to behave locally as 2D airfoils and the three dimensional effects are accounted for by the reduction of the effective AOA due to the induced flow by the wingtip vortices.

In addition to the main wing aerodynamic calculations, also the HT contribution to the aircraft aerodynamic coefficients is accounted for. The same procedure described before is used. It should be stated that, as the Ar of the HT is usually low, the assumptions made in the (LLT) do not hold. In addition to this, no downwash resultant from the main wing was considered for the HT aerodynamic calculations. These are two sources of inaccuracy of the results. Nevertheless, these inaccurate results are likely to affect both the FWG and the CMWG with the same significance, which is expected to be low due to the smaller size of the HT compared to the main wing.

Fuselage and vertical tail aerodynamics were not accounted for. These two quantities are assumed to be essentially similar for both aircraft and would have an effect on the magnitude of the L/D quantities calculated in this work and in the relative variations calculated between the FWG and CMWG. The reader should bear this in mind when analyzing the data herein.

2.3 Structures

Two different types of structures were considered for the FWG and the CMWG.

For the FWG, a wing box type of structure was parameterized in order to be suitable for optimization. The thicknesses of the upper skin, lower skin, front spar and rear spar and also the front spar and rear spar chordwise positions were allowed to vary in three stations along the half-span direction. The spanwise position of one of those stations is the wing root while the other two stations positions are also design parameters. The spanwise distribution of the thicknesses and spars positions between stations is linear. Minimum thicknesses of 0.1 mm and minimum spars distance of 1% of the local chord were assumed. See Fig. 4 below for an illustration of the wing box structure and structural variables of the FWG.

The structural part of the analyses uses these input parameters together with the airfoil chord and twist spanwise distribution and the lift distribution provided by the LLT in a specific flight condition to calculate the Equivalent Beam (EB) stiffness and mass properties of the wing structure and the stress distribution and maximum stress due to the load distribution.

For the CMWG, the load bearing structure considered is the whole wing skin. The skin thickness distribution along the airfoil contour is determined by an optimization procedure similar to the one used in Vale et al. (2011). Using this methodology, a base airfoil is slightly altered in order to separate the trailing edges of the upper and lower airfoil lines. Using actuation to reduce the distance between the upper and lower trailing edges forces the airfoil to deform, increasing its camber (see Fig. 1). Optimization can then be used to adjust as well as possible the deformed shape to a target shape which may provide aerodynamic benefits.

The maximum camber target shape was determined by imposing a cubic polynomial shape for the camber line of the airfoil and maintaining the original airfoil thickness distribution and maximum camber location. The maximum camber of the airfoil was then arbitrarily chosen to be 7% (see Fig. 2). Figure 2 shows the baseline airfoil (Selig 8052) which is used for the CMWG and the FWG, as will be discussed in the next sub-sections, and the target airfoil shape with maximum camber.

The target shape was not aerodynamically optimized for any operation condition. It was only verified that the cambered airfoils could outperform the original shapes within some C_l range at different Re of operation. It can be seen from Fig. 2 that the target shape can provide not only higher C_l values but also increase the C_l/C_d ratio for C_l values slightly over 0.5 and Re values over 60000.

For airfoil chords ranging from 2.5 cm to 12.5 cm, the structural optimization procedure was used to obtain the thickness distributions and actuation required for minimal difference between the actuated airfoil and the target shapes. Once this task was performed, the aerodynamic coefficients of the airfoil shapes resulting from different actuation values (or airfoil shape parameters) were obtained and stored as the databases to be used in the aero-structural analysis of the CMWG main wing designs.

A lower boundary of 0.1 mm was used for all thickness distributions. The objective function was the minimization of the average of the absolute difference between the actual and the target shape in several airfoil points with constraints in the maximum deviation and stress. Figure 3 shows the structural optimization results and the fully actuated shapes for different airfoil chords compared to the target shapes.

As for the FWG, the CMWG wing structure stiffness and mass properties to use in the equivalent beam model are

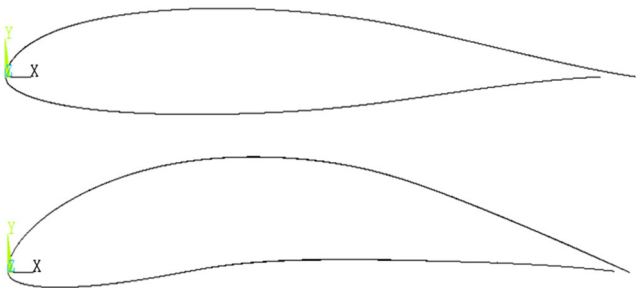

Fig. 1 Altered (*top*) and actuated (*bottom*) airfoil for camber morphing

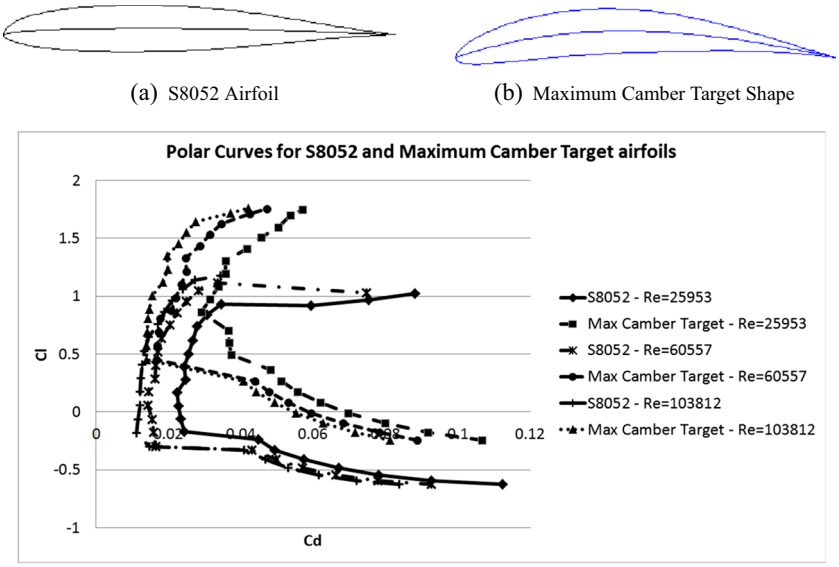

(a) S8052 Airfoil (b) Maximum Camber Target Shape

(c) Polar Curve

Fig. 2 *Top*: Original (**a**) and Target (**b**) airfoil and camber lines shapes for the CMWG. *Bottom* (**c**): Polar (C_l vs C_d) curves for the Selig 8052 airfoil and the maximum camber target shape airfoil at several Re values

calculated taking into account the thickness distribution for each wing section, obtained from the databases, based on the chord and airfoil shape parameter.

2.4 Static stability

The inclusion of the static stability in the analysis is made by simply calculating the static margin of the aircraft tacking into account the Center of Gravity (CG) position, the C_L vs AOA curve slopes of the main wing and HT and their planform areas.

2.5 MDO procedure for the FWG

The design of the FWG made here is essentially in order to provide metrics for comparison with the CMWG. In particular, it should provide a measure of the fixed wing structural mass to be compared to the morphing wing mass, which is already strongly influenced by the airfoil thickness distributions calculated to allow the camber morphing.

In addition to this, the two designs may be compared in terms of L/D performance in the design conditions and in off design conditions.

Ideally, the FWG design should provide the absolute optimal L/D ratio for the design conditions but this would imply a level of design freedom which would include complete wing surface shape and wing structure parameterization, along with powerful computational resources, not available to the authors. Instead, a constant airfoil was chosen for the FWG main wing (the Selig 8052, with 2% maximum camber and good overall performance for a wide range of C_L and low Reynolds number values, see Fig. 2) and the wing structure is a wing box parameterized as described earlier.

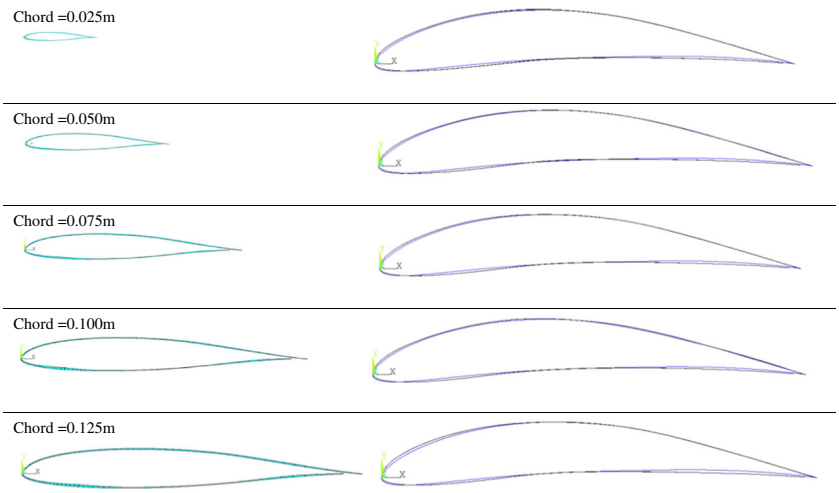

Fig. 3 *Left*: Structural optimization results (thickness distributions) for different chords. *Right*: comparison between actual (*black*) and target (*blue*) shapes

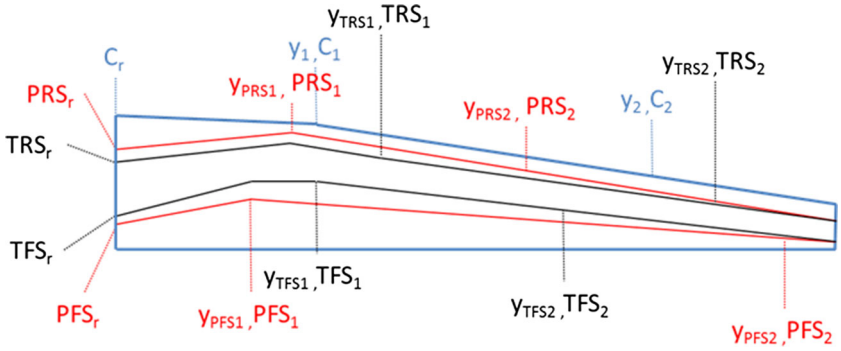

Fig. 4 Design variables for the FWG MDO problem: Chord and twist spanwise distribution variables (*blue*); Front and rear spars positions spanwise distribution variables (*red*); Front spar and rear spar thickness spanwise distributions (*black*). Twist, upper skin and lower skin thickness spanwise distributions are not shown

As a consequence, one can always argue that the benefits or penalties are relative between the FWG and CMWG designs and that no general conclusion can be drawn about the introduction of morphing in the design. In fact, one can use this argument whenever the design freedom is constrained by some reason. Nevertheless, it is the authors believe that the comparisons are reasonable and give insight on potential benefits of the usage of morphing in this case.

The goal of the design consists of trying to maximize the L/D ratio of the FWG in the design conditions of Table 1, with the design variables being the spanwise distributions of chord, twist, spars positions, spars and skin thicknesses. The constraints are related to the maximum tensile and compressive values of stress in the limit loading conditions, to the flight trimming conditions and to the local AOA for both the main wing and HT.

Figure 4 depicts the design variables. Purely structural variables in the problem are the front and rear spars positions relative to chord (PFS and PRS), the front and rear spars thicknesses (TFS and TRS) and the upper and lower skins thicknesses (TUS and TLS) in three spanwise stations (wing root, spanwise stations y_{*1} and y_{*2}) in a total of 30 variables. Variables that couple both structures and aerodynamics are the chord (C) at three different spanwise stations (root, y_{C1} and y_{C2}) and the twist (θ) at two different spanwise stations ($y_{\theta 1}$ and $y_{\theta 1}$), adding 9 more variables to the problem. As stated earlier, the spanwise distributions of the different quantities are linear piecewise.

In addition to the main wing related variables there are also the trim related variables which include the aircraft AOA, the HT chord (c_{HT}), the HT incidence angle (i) and the payload CG position in the aircraft's longitudinal axis (CGx).

The objective function of the MDO problem adopted here can be interpreted as a multi-objective function in which the improvement of flight performance represented by the L/D ratio is one objective and wing mass reduction is another. The reason behind this approach is that early optimization attempts not considering the wing weight increase as a penalty led to inferior L/D performance with excessive wing weight (as compared to the payload weight). One can think of wing mass increase correlating with initial aircraft cost increase, being the objective function an overall (operational + initial) cost representation.

Equation (1) shows the MDO problem statement.

$$
\begin{array}{ll}
\text{minimize} & f(x) = -W_1 \times L/D + W_2 \times W_{\text{wing}}/W_{\text{payload}} \\
\text{with respect to} & x = \text{(chord and twist variables, HT variables, CGx, AOA)} \\
\text{subject to trimming constraints} & \left| \dfrac{L - W\cos(D/L)}{W} \right| - 0.01 \leq 0 \\
 & \left| \dfrac{D - W\sin(D/L)}{W} \right| - 0.001 \leq 0 \\
\text{stress constraints} & \dfrac{\sigma_{\max}^{\text{pull-up}} \times SF - \sigma_{\text{yield}}}{\sigma_{\text{yield}}} \leq 0 \\
 & \dfrac{\sigma_{\max}^{\text{pull-down}} \times SF - \sigma_{\text{yield}}}{\sigma_{\text{yield}}} \leq 0 \\
\text{limit local AOA constraints} & \text{AOA}_{max}^{\text{wing}} - 10^\circ \leq 0 \\
 & \text{AOA}_{max}^{\text{HT}} - 10^\circ \leq 0 \\
\text{and static margin} & \text{SM} - 0.2 \leq 0
\end{array}
\tag{1}
$$

Figure 5 shows the data flow inside the MDO procedure. The main wing chord and twist distributions, along with the geometrical AOA, HT incidence and HT chord are used as inputs for the LLT block which outputs the total L/D, the effective AOA distributions and the C_{L_α} slopes for both the main wing and the HT, at the design flight conditions.

The C_{L_α} slopes, the wing and HT areas and their mean aerodynamic chords (calculated based on the geometrical inputs) are then used for the static margin calculation in the present flight condition.

Changing the flight condition to the limit load flight condition (maximum velocity and maximum and minimum AOA) the LLT block is used to obtain the lift distribution in both load cases, which in turn is used as input together with the variables affecting the structural properties to the EB block, which outputs the wing structural weight and the maximum absolute values of stress for the two limit load cases.

As shown in Fig. 5, the various outputs are then used for the objective function and constraints calculations, suitable for usage with an optimization algorithm. The fmincon function in Matlab™ with the interior-point algorithm was used to perform every optimization reported in this work.

In order to generate a Pareto Front of L/D versus Wing weight, the objective function weight parameters W_1 and W_2 were varied within the range [0.01, 0.1] and [0.0, 1.0] respectively, and the MDO procedure was performed for each pair (W_1, W_2). Results are shown in the following sections.

2.6 MDO procedure for the CMWG

For the CMWG, an altered airfoil based on the Selig 8052 was chosen in order to maintain comparability with the FWG. The idea was to allow the CMWG to have a similar performance to the FWG one and explore the morphing capability in off-design flight conditions. The main difference between the two is that the unactuated morphing wing presents constant zero twist distribution along the span, therefore preventing a very close match between the two wing configurations.

The twist behavior in a wing with this type of camber morphing concept can be described as following: if all wing sections are actuated in order to obtain the same relative camber along the span, the wing will remain untwisted; if the actuation increases camber towards the tips, the wing twist increases towards the tip, i.e. increasing local AOA towards the tip) and vice versa; if the wing chord is tapered the actuation effects in the twist distribution are magnified. The camber and twist of the morphing wing are therefore coupled.

In fact, the twist distribution is not known *a priori* given a chord distribution and the morphing airfoils actuation distribution. It could be evaluated using a FE model analysis within the MDO algorithm but the computational cost would be prohibitive.

An initial approach to tackle this issue was to discard chord tapering effects on twist variation and assume the airfoil sections to behave as 2D structures. This way, the twist distribution along the span is assumed to depend solely on the actuation distribution and can be previously calculated to create databases for interpolation using the FE models obtained from the thickness distribution optimizations shown in Fig. 3, assuming the leading edge as the point of rotation of the wing sections.

Although not extremely accurate, this approach allows the optimization procedure to obtain candidate configurations for the chord distribution with acceptable L/D and

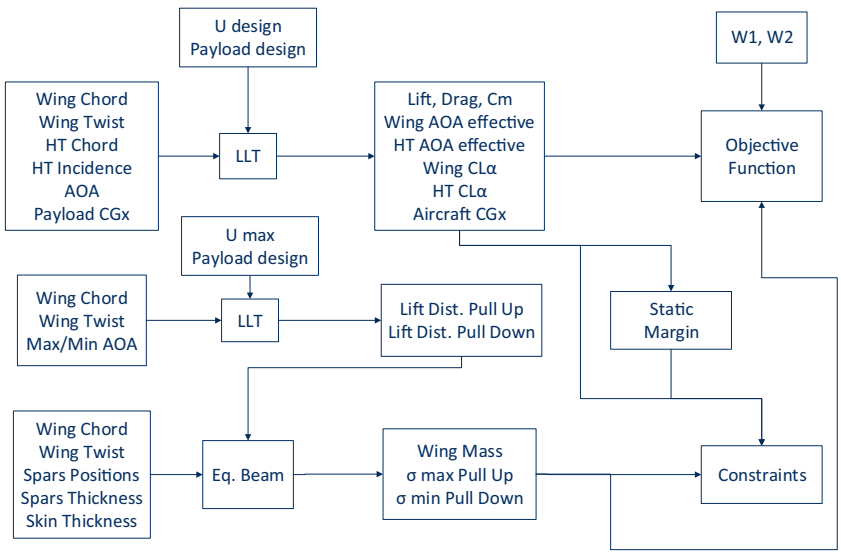

Fig. 5 Data flow for Objective Function and Constraints calculation during the FWG MDO procedure

wing weight value to proceed with the CMWG design. The optimization statement is shown in equation (2).

$$
\begin{array}{ll}
\text{minimize} & f(x) = -W_1 \times L/D + W_2 \times W_{\text{wing}}/W_{\text{payload}} \\
\text{with respect to} & x = \text{(chord and actuation variables, HT variables, CGx, AOA)} \\
\text{subject to trimming constraints} & \left| \dfrac{L - W\cos(D/L)}{W} \right| - 0.01 \leq 0 \\
 & \left| \dfrac{D - W\sin(D/L)}{W} \right| - 0.001 \leq 0 \\
\text{limit local AOA constraints} & \text{AOA}_{max}^{\text{wing}} - 10^\circ \leq 0 \\
 & \text{AOA}_{max}^{\text{HT}} - 10^\circ \leq 0 \\
\text{and static margin} & \text{SM} - 0.2 \leq 0
\end{array}
\tag{2}
$$

This procedure is depicted in Fig. 6 and similarly to the FWG MDO procedure and it is run for several pairs of objective function weights (W_1, W_2). The main differences between the FWG and the CMWG MDO procedures is that the wing twist is substituted by the actuation distribution and the stress constraints are not applied in this initial design step.

Having the chord distribution for the interesting configuration candidates (candidates with L/D values higher than the FWG and lower wing weight), another optimization procedure is used to obtain the wing actuation distribution in the limit load cases.

The expected benefit in the wing structure weight is originated in this stage of the design. Due to the character of the camber morphing concept applied in this case, it seems potentially beneficial if the wing can itself limit the loading it is subjected to by changing the lift distribution along the span. This way, a flight condition that produces a high load factor in a fixed wing configuration can be flown if the loading is relieved by camber distribution rearrangement, reducing the load factor. Furthermore, if the loading is redistributed towards the root of the wing, significant reductions in root bending moment can be achieved with consequent structural mass reduction.

Since the present morphing concept is a camber increase concept, it is easier for the CMWG to increase the wing loading (which in a pull down maneuver means decreasing the absolute value of wing load) that to reduce it. Therefore,

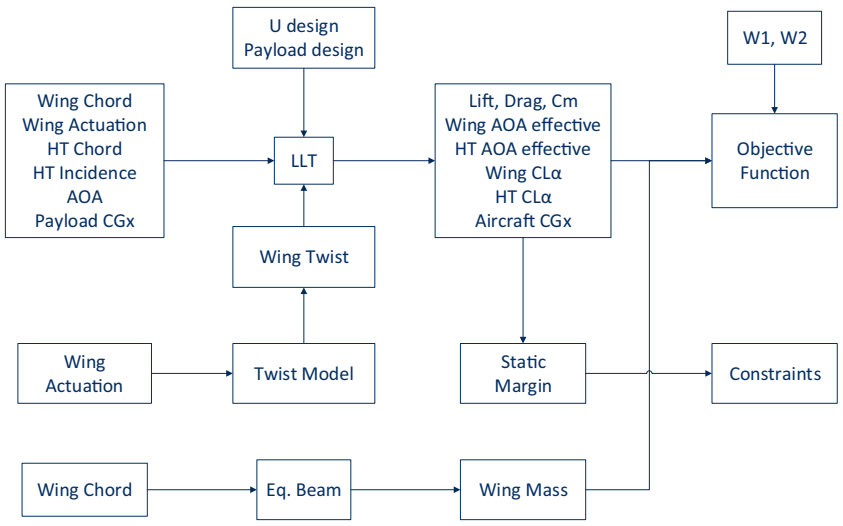

Fig. 6 Data flow for Objective Function and Constraints calculation during the chord distribution of CMWG optimization procedure

the wing is less prone to reduce positive load factors than to increase negative load factors. For this reason, the optimization objective function in this stage is to maximize the positive load factor in the pull up maneuver (for maximum maneuverability) while constraining negative load factor in the pull down maneuver to −3 g (guaranteeing a minimum level of maneuverability in pull down maneuvers).

This time the FE model of each candidate wing configuration is generated and a database of the twist distribution on 41 points along the span for a sample of 125 different actuation distributions was calculated. A surrogate model is generated with the calculated sample using the Kriging method (Lophaven et al. 2002) with a linear correlation for the stochastic part and a 0 degree polynomial for the deterministic part.

This model is then used during the optimization procedure to determine the actuation distributions that reduce the loading on the wing in order to keep the structure stress within the allowable limits. At the end of this optimization procedure, the FE model is analyzed with the actuation distributions calculated and the differences between the twist distributions calculated from the FE model and the surrogate model are evaluated. If these are considered excessive (the square root of the mean square error in the 41 points >1%) the sample is increased with the FE model results and the optimization procedure is performed again. Otherwise, the configuration is considered valid.

Figure 7 depicts the data flow in the optimization and surrogate model update procedures described above and equation (3) shows the optimization statement.

minimize	$f(x) = -L/W_{\text{payload}}$	
with respect to	$x =$ (actuation variables)	
subject to negative load factor constraint	$\left(\frac{L}{W}\right)^{pull-down} + 3 = 0$	(3)
stress constraints	$\frac{\sigma_{\max}^{\text{pull-up}} \times SF - \sigma_{\text{yield}}}{\sigma_{\text{yield}}} \leq 0$	
	$\frac{\sigma_{\max}^{\text{pull-down}} \times SF - \sigma_{\text{yield}}}{\sigma_{\text{yield}}} \leq 0$	
limit local AOA constraints	$\text{AOA}_{max}^{\text{wing}} - 10^\circ \leq 0$	

Finally, for the valid configurations, the actuation distribution is calculated in order to obtain the maximum L/D, in the design conditions using the same sample updating scheme as described before. Equation (4) shows the optimization statement and Fig. 8 summarizes the complete procedure for the design of the CMWG.

minimize	$f(x) = -L/D$	
with respect to	$x =$ (actuation variables, HT variables, CGx, AOA)	
subject to trimming constraints	$\left\lvert \frac{L - W\cos(D/L)}{W} \right\rvert - 0.01 \leq 0$	(4)
	$\left\lvert \frac{D - W\sin(D/L)}{W} \right\rvert - 0.001 \leq 0$	
limit local AOA constraints	$\text{AOA}_{max}^{\text{wing}} - 10^\circ \leq 0$	
	$\text{AOA}_{max}^{\text{HT}} - 10^\circ \leq 0$	
and static margin	$\text{SM} - 0.2 \leq 0$	

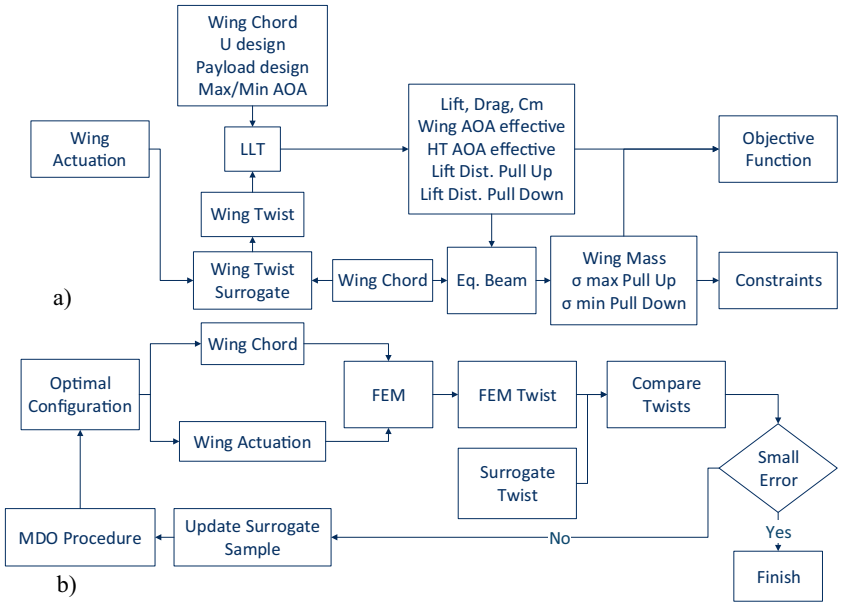

Fig. 7 Data flow for calculations during the actuation distribution of CMWG optimization procedure: **a** Objective Function and Constraints; **b** Surrogate and FEM twist results comparison and Surrogate model update procedure

3 Results

In this section, the results of the design of the FWG and the CMWG are presented with focus on the geometry and structure of the aircraft.

3.1 FWG design

The MDO procedure applied during the FWG design produced 110 designs which are represented in the Pareto Front depicted in Fig. 9. It can be seen that although a decrease in wing mass tends to increase the L/D ratio, the two parameters do not show linear correlation. In fact, the maximum L/D design is not the one corresponding to the lowest wing mass.

Despite the existence of other designs potentially interesting due to their L/D values (different markers' shape) near the maximum and lower wing mass values, the design chosen was the one providing the maximum L/D and marked with a cross in Fig. 9 (design ID 56). This choice will condition the conclusions that can be drawn when comparing with the CMWG, and the reader should bear in mind that this study is made as if the operational performance is preferred over the initial cost.

Table 2 compares the best configurations in terms of some of the design parameters. It can be noticed that significant reductions in wing mass can be achieved if one is willing to jeopardize the L/D performance in a small amount. This illustrates the point discussed in the previous paragraph and the implied relativity in classifying a configuration as optimal.

The L/D ratio shows clearer trends with other design parameters, as depicted in Fig. 10 below. The trends are to move the payload CG (and therefore the aircraft CG) downstream in order to increase the lift produced by the horizontal tail necessary for trimming the aircraft, up to near the AOA of best L/D of the HT.

The maximum stress in the designs also increases as the wing mass decreases as expected (see Fig. 11), although in the best designs the constraint is not active. In these cases the maximum stress is near the limit, as can be seen in Table 2.

The chosen wing design geometry and structural parameters distributions are depicted in Fig. 12 for half the span of the wing. The operation AOA is 6.83 degrees.

The chosen configuration presents two linear segments in every parameter distributions, meaning that the number of design variables could be increased in order to allow greater freedom in the design. Nevertheless, early optimizations did not show that this additional freedom would bring significant benefits to the design. Due to the increase in

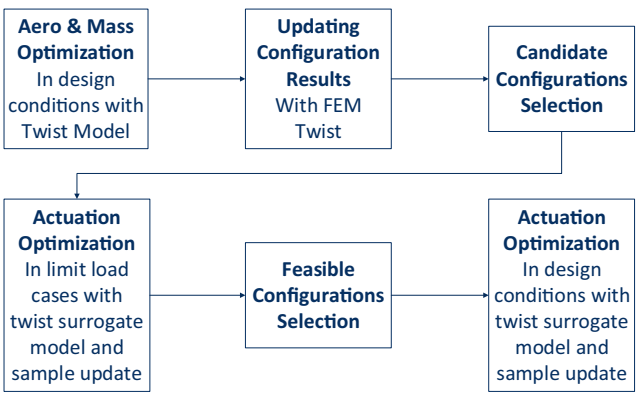

Fig. 8 Summary of the MDO procedure for the design of the CMWG

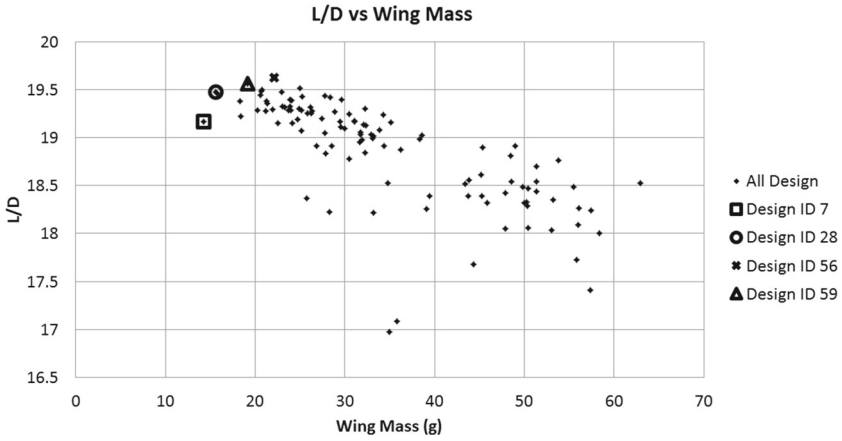

Fig. 9 L/D vs Wing Mass Pareto Front results from the MDO of the FWG

computational time implied, the number of design variables was kept as reported before.

The optimal design shows a planform with nearly constant chord from the root to more than half of the half span of the wing, followed by a tapered section towards the wing tip. The twist has a negative slope from the root to nearly half the half span and a positive slope from there to the tip, although remaining negative throughout the span. These two distributions (chord and twist) are responsible for the effective AOA, lift, drag and pitching moment coefficient distributions along the wing span in the design conditions and are depicted in Fig. 13.

Since viscous drag is also accounted for in the analysis, the drag distribution is a compromise between induced drag reduction and viscous drag increase due to the reduction in local Re number towards the tip. The resulting lift distribution is therefore close to elliptical and one can notice from Fig. 13 the effective AOA varying between 5.45 and 3.92 degrees up to very near the wing tip, keeping the wing airfoil sections working close to the maximum L/D AOA for the local Re number.

In the tapered wing section, the C_d increases towards the tip as a consequence of the Re number decrease and, although the chord reduction partially compensates and reduces the local drag, the local L/D is degrading towards the tip.

Table 2 Parameters of the selected MDO designs for the FWG

Design ID	7	28	56	59
L/D	19.17	19.48	19.627	19.566
$\Delta L/D$ (%)	−2.33	−0.75	0.00	−0.31
Wing Mass (g)	14.291	15.623	22.084	19.137
Δ Wing mass (%)	−35.29	−29.26	0.00	−13.34
HT chord (m)	0.102	0.100	0.100	0.102
HT AOA (deg)	4.76	4.83	4.92	4.92
Payload CGx (m)	0.096	0.097	0.099	0.100
Max Stress criteria (%)	97.39	97.19	93.55	97.23

The results obtained for the structural design variables determine the wing mass and the stress distribution along the span, which is depicted in Fig. 14.

The wing structure is determined by the pull up load case, which is not surprising since the airfoil chosen is cambered and the pull up and down cases were defined with +/−10 degrees of AOA. The positive AOA load case then produces higher lift due to the airfoil camber and consequently higher stress values. Besides this, the stress distribution is similar in both cases.

One can observe that the structure may be considered highly stressed, with a significant extent of the wing span with stress levels near the allowable limit. The achieved load factors in the pull up and down load cases are +13.51 g and −8.18 g, respectively.

Finally, the FWG design has an Ar of 11.74 and a mean aerodynamic chord of 8.52 cm.

3.2 CMWG design

The CMWG design, being the result of a MDO architecture based on sequential optimization, presents itself as a set of feasible final results. In fact, the design presented below was the only one for which convergence was achieved in every step of the design. From the first design stage (determination of the chord distribution), 4 designs where candidates with higher L/D and lower wing mass than the FWG design and from that set only one design was able to withstand the loads for the pull up and down maneuvers.

Figure 15 depicts the CMWG configuration for the design flight conditions. The actuation parameter distribution here represents the fraction of the distance between upper and lower trailing edges that is reduced during actuation. A 0 value corresponds to the unactuated state and

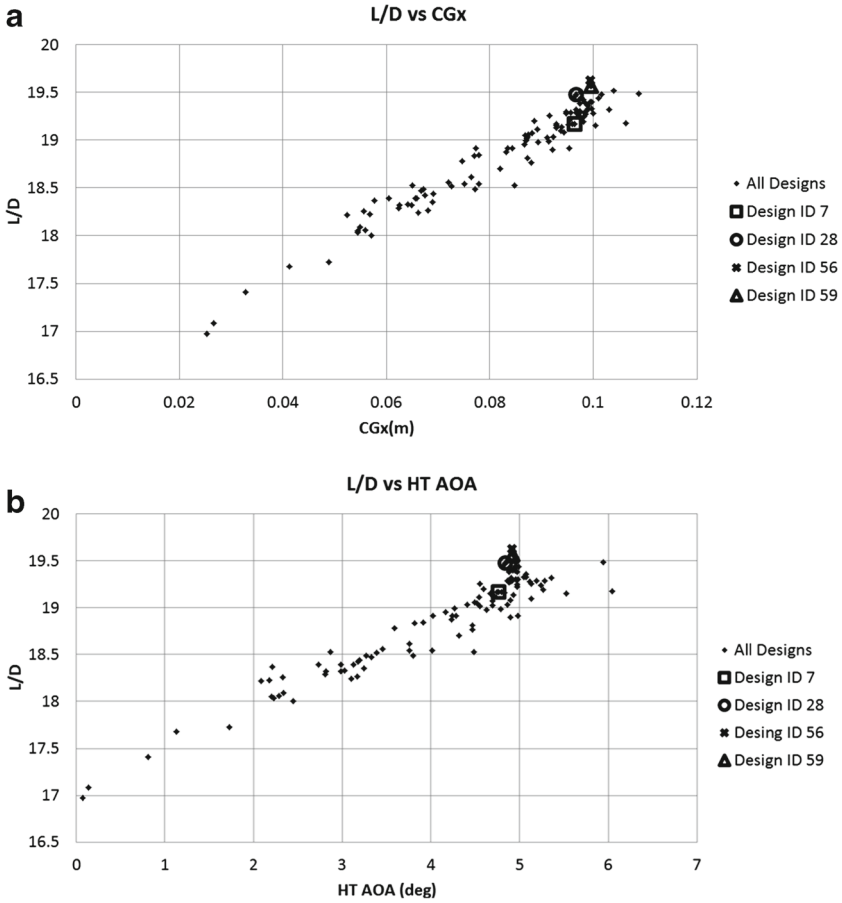

Fig. 10 L/D variations with the design parameters: L/D vs Payload Position (**a**) and L/D vs HT AOA (**b**)

a range between 0.563 and 0.601 corresponds to the fully actuated state, depending on the local chord, representing roughly to 7% camber. The twist distribution is obtained from a surrogate model matching the FE model results closely, as explained earlier.

In Fig. 16 the FE model of the CMWG is shown, together with the stress intensity and a detail of the twist at the wing tip. One can observe that the stress intensity due to actuation only is very low (5.4 MPa) and that the wing twist rotation line is very near the leading edge

Figure 17 depicts the aerodynamic parameters distributions resulting from the analysis in the design flight conditions and optimal configuration of the CMWG. Comparatively to the FWG results, the CMWG wing operates

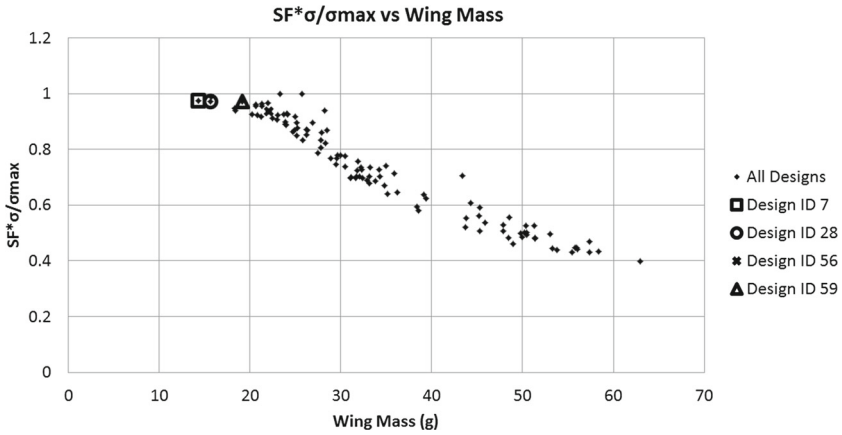

Fig. 11 Maximum Stress Criteria vs Wing mass for the various designs

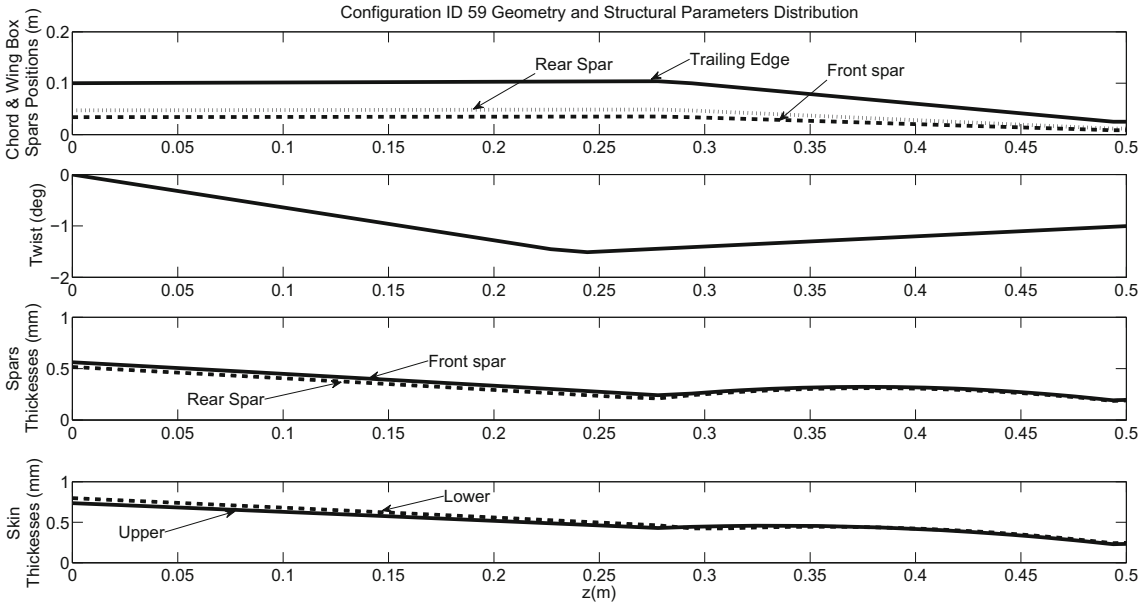

Fig. 12 Chosen configuration geometry and structural parameters distributions

with higher local C_l and slightly higher local AOA values near the root and lower near the tip. It also produces higher local pitch down moment coefficient. The l, d and l/d distribution shows very similar values, when compared with the FWG.

Therefore, it is not surprising that the L/D performance of the two wings is so close (19.63 for the FWG and 19.66 for the CMWG).

The limit load cases analyses results are depicted in Fig. 18. For the pull up maneuver, it is noticeable the maximal actuation in the root and minimum actuation at the break station and tip, in order to produce a negative twist in the wing and therefore reducing the local AOA and the lift production towards the tip. The load distribution then becomes more intense near the root contributing to the reduction of the root bending moment. The maximum

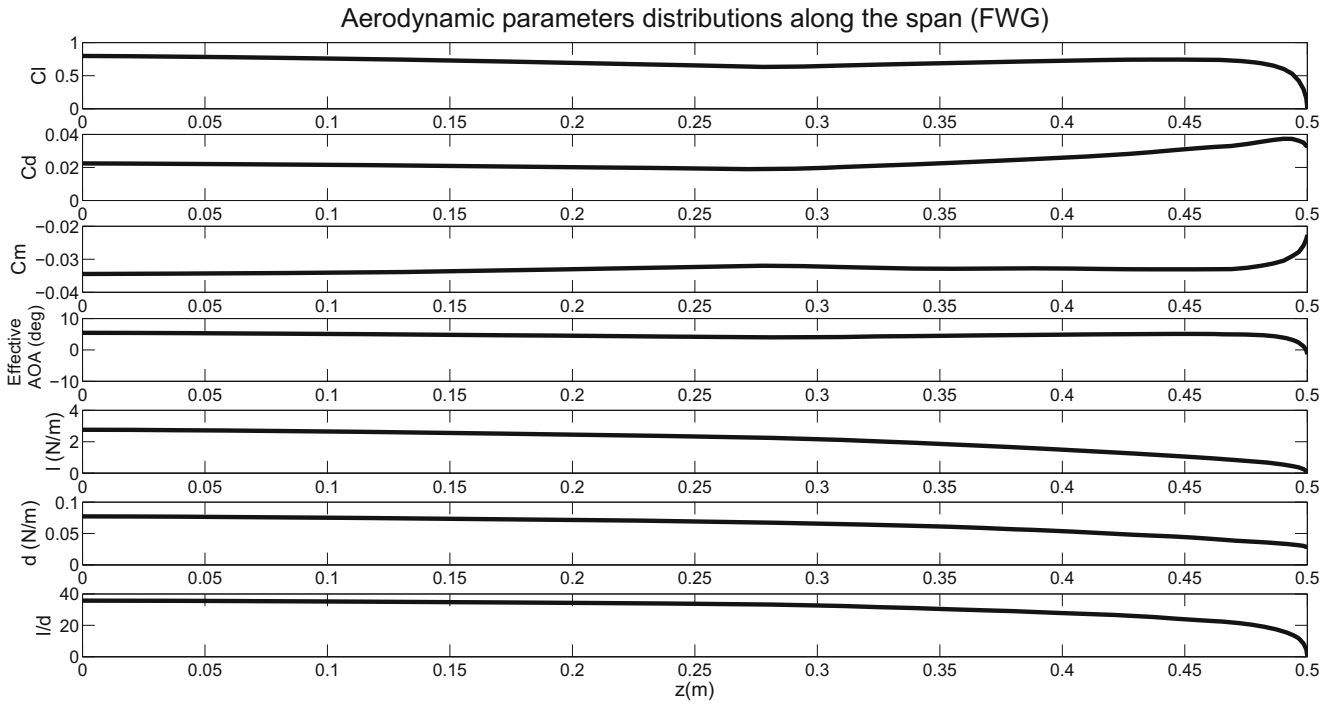

Fig. 13 Aerodynamic parameters distributions along the span for the optimal design of the FWG

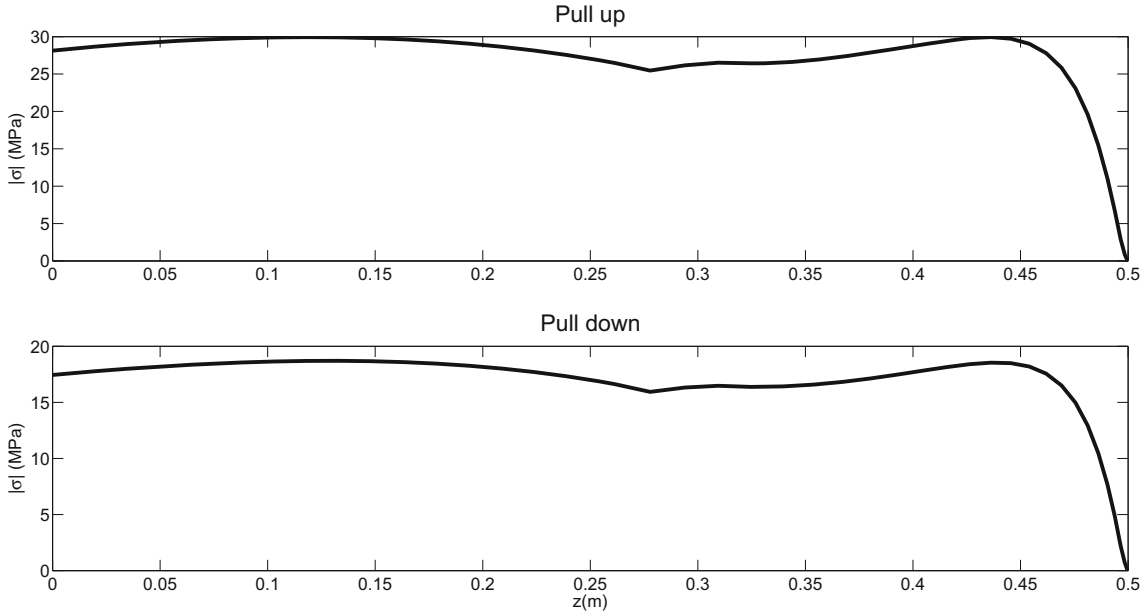

Fig. 14 Maximum absolute values of bending stress distributions in the limit load cases for the FWG

load factor obtained in this situation is 7.24 g. For the pull down maneuver, which is constrained to a load factor of −3 g, it can be seen the actuation first increasing with higher slope towards the tip in order to increase both camber and twist and then increasing with a lower slope which still increases the camber but decreases the twist. The overall effect decreases the magnitude of the lift production.

4 Structural and performance comparisons

Table 3 compares the FWG and CMWG some design and performance parameters in the design flight condition.

The two configurations produce similar L/D values and similar HT incidence and configuration, suggesting that HT weight and trim requirements are similar with slight disadvantage to the CMWG.

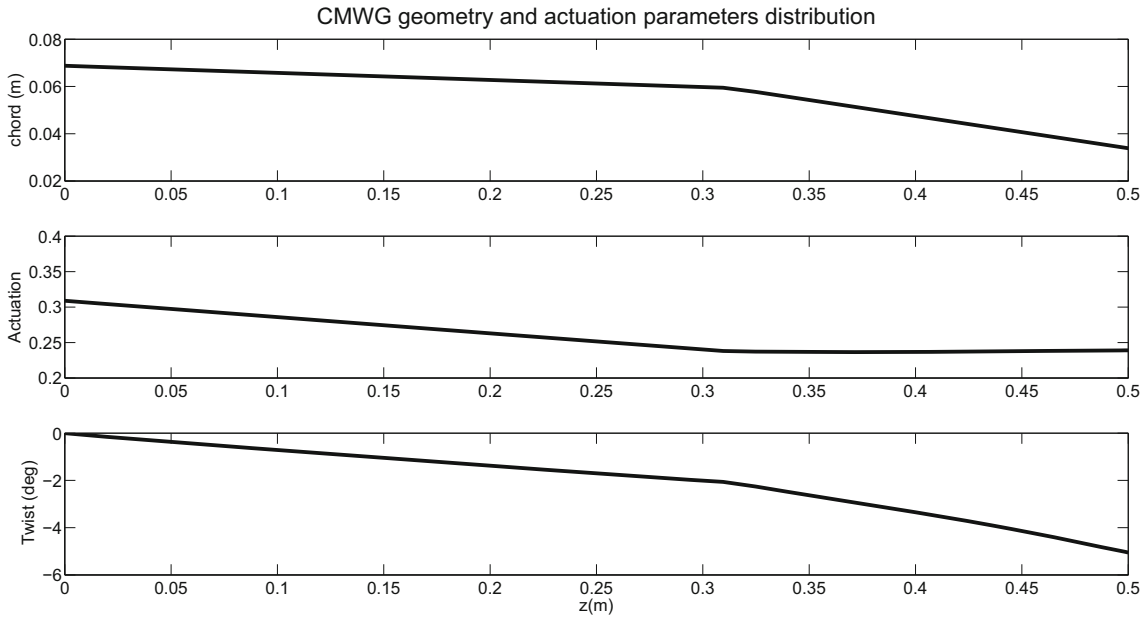

Fig. 15 Chord (*top*), Twist (*bottom*) and Actuation parameter (*middle*) distributions for the CMWG at the design flight conditions

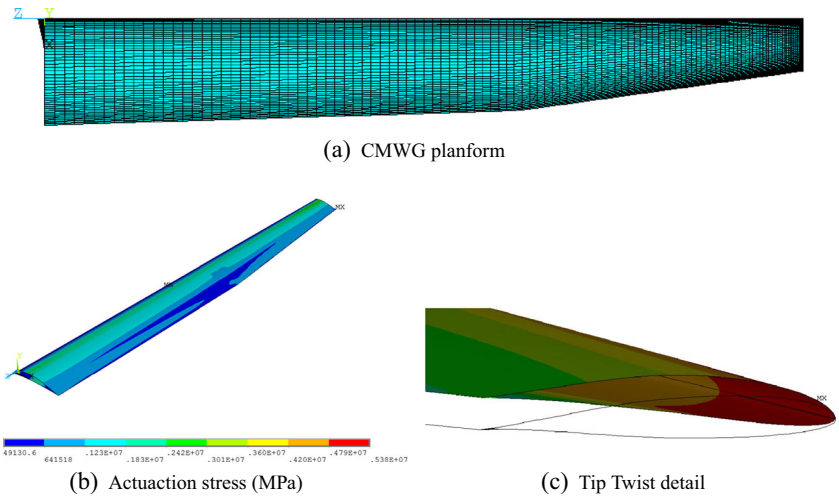

(a) CMWG planform

(b) Actuaction stress (MPa)

(c) Tip Twist detail

Fig. 16 **a** Planform detail of the FE model; **b** Actuation stress intensity in design configuration conditions; and **c** detail of the tip airfoil twist compared to the unactuated position

Differences can be seen in wing area, Ar, AOA and mass. The CMWG wing is significantly more slender and the reason for this is that the already prescribed thickness distributions for camber morphing cause a mass increase that has to be compensated by a mean aerodynamic chord reduction in order for the CMWG to be competitive in terms of wing structural mass. In turn, this lower mean chord reduces the operation Re with the effect of decreasing the l/d values of the unactuated wing, which are then compensated by morphing the wing camber and twist. A slightly lower wing mass and a higher operation AOA are the outcomes of these trade-offs.

If the FWG configuration chosen had been any other design from Table 2, the benefits in wing structural mass described here would become penalties but also the benefits in L/D would become more significant. Another remark should be made about the load factors, to which the structural mass is related. The CMWG is able to comply with the requirements at the expense of maneuverability. In this case, the pull up radius of the FWG (5.72 m) is little more than half of the CMWG one (9.80 m).

Figures 19 and 20 show the L/D and vertical speed values for a range of different payload values and several flight velocities respectively. Here the greatest advantage of the

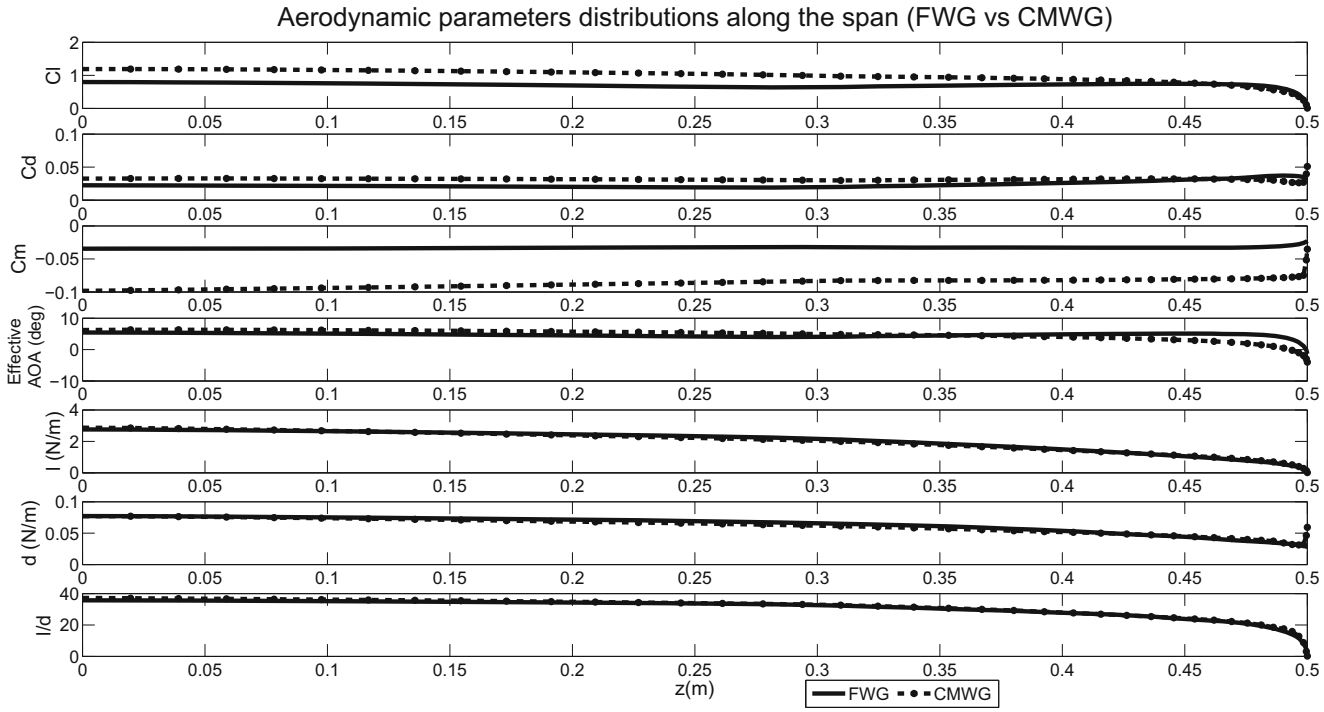

Fig. 17 Aerodynamic parameters distributions along the span for the optimal design of the CMWG in comparison with the FWG

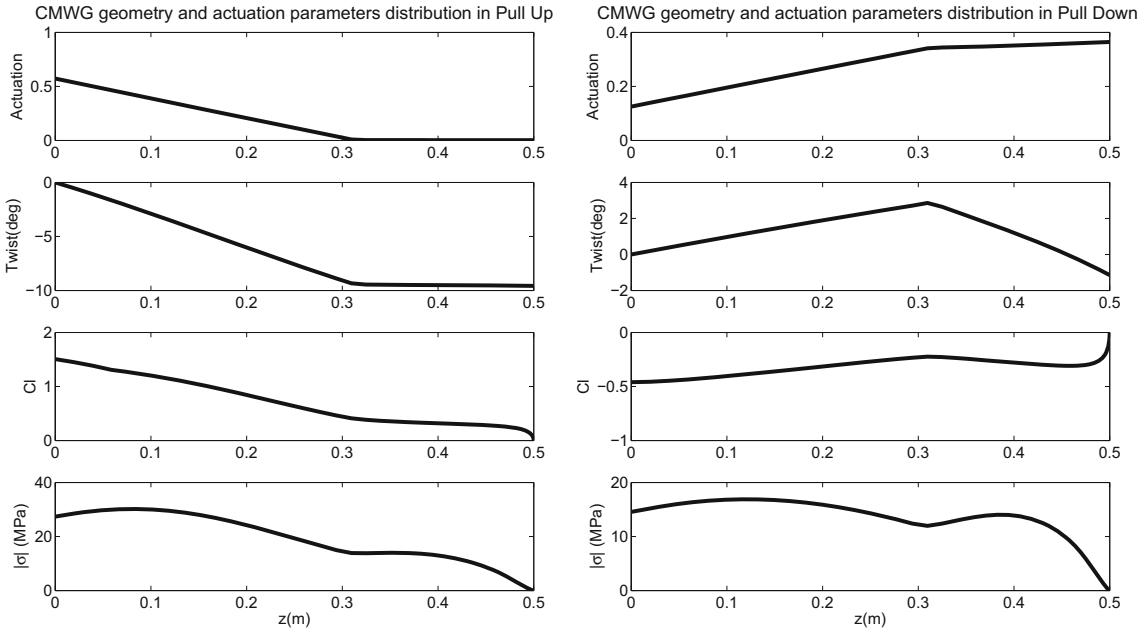

Fig. 18 Actuation, twist, Cl and bending stress value distributions along span for the CMWG in pull up (*left*) and pull down (*right*) conditions

morphing concept can be observed with the CMWG being able to significantly outperform the FWG in a wide range of flight conditions with slight penalties in L/D in a small range of low speeds for each different payload value. The small scatter in the data of the CMWG is the result of finding a local minimum during the configuration optimization in some flight conditions.

The penalties in L/D at low speeds are essentially caused by the comparatively lower local Re and higher AOA of operation of the CMWG relatively to the FWG. As speed increases and the Re effects become less important and the AOA is reduced, the wing's lower wing area and morphing capability allow the aircraft to achieve higher L/D values. Range is therefore augmented with the CMWG.

The vertical speed versus horizontal speed plot in Fig. 20 shows also benefits in the same flight conditions as before. Nevertheless, the minimum vertical speed occurs in the speed range where the CMWG shows penalty relatively to the FWG. The resulting penalties in maximum endurance are small, varying between 1.4% and 2.3% in the payload and flight conditions analyzed.

Finally, Fig. 21 presents the configurations of the CMWG in a low payload-high speed condition, the maximum L/D with the design payload condition and in a high payload-low speed condition.

In the high speed-low weight condition, the actuation magnitude is very small, only enough to generate some negative twist of small magnitude towards the tip, as could be expected since the operating C_L is very small.

The best L/D with the design payload presents a small actuation level in the wing root which is reduced towards the tip, resulting in a negative twist of about -3 degrees at the tip. This configuration produces an elliptical lift distribution.

The low speed-high weight condition, due to the high C_L requirement, has maximum actuation at the wing root and reduces it up to the break station of the wing. This reduces the local AOA of the wing sections starting from the root to the break station, which otherwise would be excessively high producing excessive drag. From the break station to the tip, the actuation increases in order to compensate the tapper effect in the twist and produce more lift.

Table 3 Parameters of the FWG and CMWG in the design flight condition

Parameter	FWG	CMWG
Wing Mass (g)	22.08	19.94
HT chord (m)	0.100	0.108
HT AOA (deg)	4.92	5.08
CGx (m)	0.099	0.101
AOA (deg)	6.83	8.06
Wing Area (m^2)	0.0852	0.0575
Ar	11.74	17.38
L/D	19.63	19.66
Max Load Factor (g)	13.51	7.24
Min Load Factor (g)	-8.18	N. A

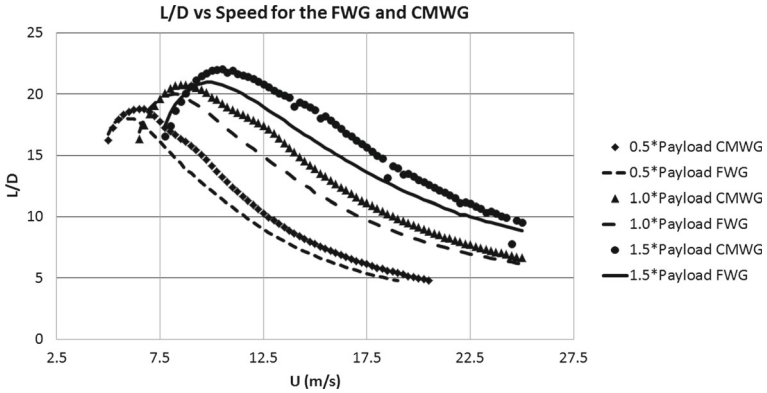

Fig. 19 L/D variation with flight speed for the FWG and the CMWG with different payload weights

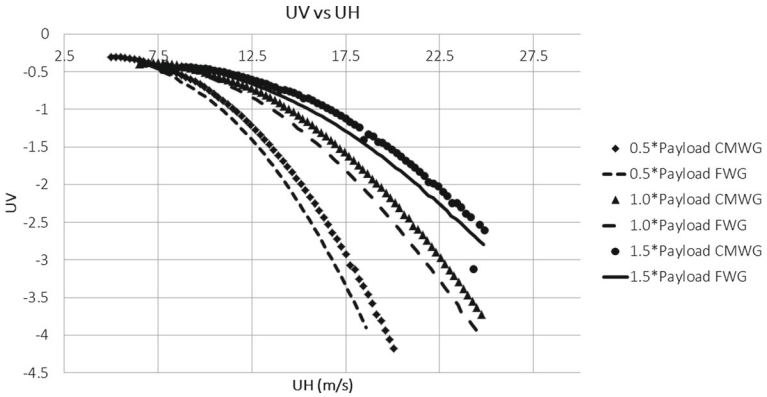

Fig. 20 Vertical speed versus horizontal speed for the FWG and the CMWG with different payload weights

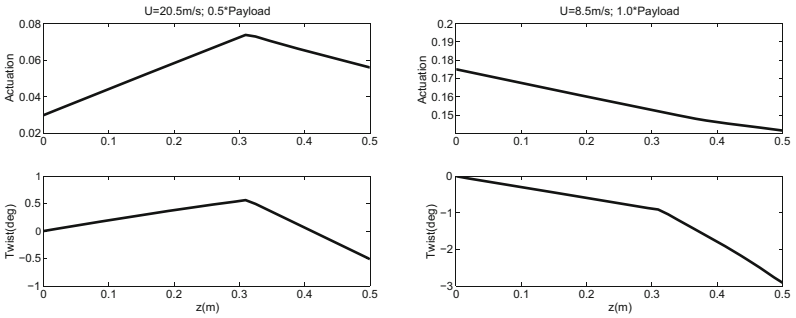

(a) Low weight-high speed condition (b) Max L/D speed with design payload condition

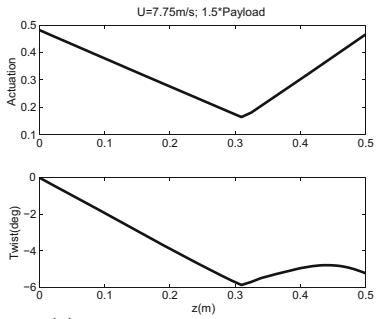

(c) High weight-low speed condition

Fig. 21 Actuation and Twist distributions for the CMWG with different payload and speed conditions: **a** Low weight-high speed condition; **b** Max L/D speed with design payload condition; and **c** High weight-low speed condition

5 Concluding remarks

The present work presents a comparison of aerodynamic and structural performance between two aircraft glider wing designs for optimal load alleviation using MDO procedures. The baseline configuration is a fixed geometry wing which is compared to the wing with camber morphing capability, with the objective to explore the camber morphing solution in terms of aerodynamic and structural performance improvement and load alleviation capability.

The camber morphing concept proposed has a coupled effect of changing the wing twist, and these variations are not known *a priori*. Therefore, and in order to keep the computational solution tractable, the CMWG MDO procedure was based on sequential optimization while the FWG MDO procedure was based on a single level optimization.

In terms of load alleviation and structural benefits obtained by the CMWG in comparison with the FWG, it is observed that the CMWG can effectively reduce the magnitude of the load factor experienced by the aircraft, thus allowing its structure to withstand the loads at lower weight. The main drawback is the loss of maneuverability of the aircraft, which is an inherent characteristic in load alleviation. From a structural perspective, the requirement for a structure capable of camber morphing prevents the design of an efficient structure to withstand the loading.

The performance comparison was done essentially in terms of L/D, or range and endurance. When considering the range metric, the CMWG is able to provide higher maximum L/D and higher L/D over a wide range of flight speeds and payload values. Its lower mean aerodynamic chord, resulting from the multi-objective function of the MDO procedure in order to reduce wing mass and its camber adaptability allow the CMWG to maintain higher L/D values compared to the FWG throughout the payload and speed envelope.

At low speeds, the L/D of the CMWG is slightly lower than the FWG L/D, and this relates directly with the magnitude of the vertical speed and the maximum endurance, which is reduced by 2.3% or less. High AOA and Re effects have a strong influence in this result.

Summarizing, while achieving a very significant load alleviation, camber morphing structures are likely not to present significant structural weight reductions due to their inefficient load bearing capability. One can also conclude that while not providing significant weight reduction, the camber morphing concept provides significant aerodynamic benefits for most of the flight conditions.

The paper sheds some light on the load alleviation that can be achieved using a camber morphing concept, and the findings depend on the design goals of the FWG and the extent of its off-design operation, as well as on the design envelope which is always restricted to some extent.

Acknowledgments This work was supported by FCT, through IDMEC, under LAETA, project UID/EMS/50022/2013.

References

Cesnik CES, Last HR, Martin CA (2004) A framework for morphing capability assessment. In: Proceedings of 45th AIAA/ASME/ASCE/AHS/ASC structures, structural dynamics & materials conference. Palm Springs, California, USA. AIAA paper 2004–1654

Cooper JE, Chekkal I, Cheung RCM, Wales C, Allen NJ, Lawson S, Peace AJ, Cook R, Standen P, Hancock SD, Carossa GM (2015) Design of a morphing wingtip. J Aircr 52(5):1394–1403

Dayyani I, Friswell MI (2016) Multi-objective optimization for the geometry of trapezoidal corrugated morphing skins. Struct Multidiscip Optim:1–15

De Gaspari A, Ricci S, Antunes A, Odaguil F, Lima G (2014) Application of active camber morphing concept to a regional aircraft. In: Proceedings of the 22nd AIAA/ASME/AHS adaptive structures. National Harbor, Maryland, USA. AIAA paper 2014–1259

Drela M (1989) XFOIL: an analysis and design system for low reynolds number airfoils. Springer, Berlin, Heidelberg, pp 1–12

Falcão L, Gomes AA, Suleman A (2011) Aero-structural optimization of a morphing wingtip. J Intell Mater Syst Struct 22(10):1113–1124

Haftka RT (1977) Optimization of flexible wing structures subjected to strength and induced drag constraints. AIAA J 14(8):1101–1106

Hepperle M (2007) Javafoil. http://www.mh-aerotools.de/airfoils/javafoil.htm. Accessed: 2016-07-30

Houghton EL, Carpenter PW (2001) Aerodynamics for engineering students, 5th edn. Butterworth Heinmann, Oxford

Lophaven SN, Nielsen HB, Søndergaard J (2002) Dace: a matlab kriging toolbox. Tech. Rep. Version 2.0, Technical University of Denmark

Mangalam S, Mangalam A, Flick P (2008) Unsteady aerodynamic observable for gust load alleviation and flutter suppression. In: 26th AIAA applied aerodynamics conference, guidance, navigation, and control and co-located conferences. Honolulu, Hawaii, USA. AIAA Paper 2008–7187

Matsuzaki Y, Ueda T, Miyazawa Y, Matsushita H (1989) Gust load alleviation of a transport-type wing - test and analysis. J Aircr 26(4):322–327

Molinari G, Quack M, Dmitriev V, Morari M, Jenny P, Ermanni P (2011) Aero-structural optimization of morphing airfoils for adaptive wings. J Intell Mater Syst Struct 22(10):1075–1089

Pecora R, Amoroso F, Lecce LL (2012) Effectiveness of wing twist morphing in roll control. J Aircr 49(6):1666–1674

Regan CD, Jutte CV (2012) Survey of applications of active control technology for gust alleviation and new challenges for lighter-weight aircraft. Tech. Rep. NASA/TM 2012-216008, NASA

Santos P, Sousa J, Gamboa P (2015) Variable-span wing development for improved flight performance. J Intell Mater Syst Struct. Online Available

Shao K, Wu Z, Yang C, Chen L, Lv B (2010) Effectiveness of wing twist morphing in roll control. J Aircr 47(3):1666–1674

Vale J, Leite A, Lau F, Suleman A (2011) Aero-structural optimization and performance evaluation of a morphing wing with variable span and camber. J Intell Mater Syst Struct 22(10):1057–1073

Werter N, Sodja J, Spirlet G, De Breuker R (2016) Design and experiments of a warp induced camber and twist morphing leading and trailing edge device. In: Proceedings 24th AIAA/AHS adaptive structures conference. San Diego, California, USA. AIAA paper 2016-0315

Wittmann J (2014) Methodology for benefit assessment of morphing aircraft. Verlag Dr. Hut

Yoon HS (2013) Optimal shape control of adaptive structures for performance maximization. Struct Multidiscip Optim 48(3):571–580